

Formation of laterally ordered arrays of noble metal nanocavities for SERS substrates by using interference photolithography

V.A. Dan'ko¹, I.Z. Indutnyi¹, V.I. Mynko¹, P.M. Lytvyn¹, M.V. Lukaniuk¹, H.V. Bandarenka², A.L. Dolgyi², S.V. Redko²

¹V. Lashkaryov Institute of Semiconductor Physics, National Academy of Sciences of Ukraine
41, prospect Nauky, 03680 Kyiv, Ukraine

²Belarusian State University of Informatics and Radioelectronics,
6, P. Brovki str., 220013 Minsk, Belarus

Abstract. Using laterally ordered arrays of noble metal nanocavities as SERS substrates has been examined theoretically and experimentally. Simulation of the distribution of the electric field at the surface of nanostructures (nanocavities) has been carried out. The simulation results showed that cavities can be formed not only in a metal layer but in semiconductor or dielectric layers and then covered with a layer of a plasmon-supporting metal (silver or gold) 20...100-nm thick. In our work, chalcogenide glass has been used as a relief-forming layer. This paper presents the results of development and optimization of processes providing formation of SERS substrates as two-dimensional arrays of noble metal nanocavities by using interference photolithography based on a two-layer chalcogenide photoresist. Prototypes of SERS substrates were made as substrates with different spatial frequencies (from 1200 to 800 mm⁻¹) and depths of nanocavities (from 250 up to 500 nm). It was shown that the use of such nanocavities with the sizes larger than 500 nm enables to efficiently analyze the structure of macromolecules by using surface-enhanced Raman light scattering spectroscopy, since these macromolecules completely overlap with the regions of enhanced electric field inside the nanocavities. Technology of interference lithography based on two-layer chalcogenide photoresists makes it possible to form effective SERS substrates in the form of laterally ordered arrays of nanocavities with specified morphological characteristics (spatial frequency, nanocavity sizes, composition and thickness of a conformal metal coating) for detecting high-molecular compounds.

Keywords: SERS, interference lithography, chalcogenide photoresist, noble metal nanocavities.

<https://doi.org/10.15407/spqeo24.01.048>

PACS 81.16.Nd, 81.16.Rf, 82.80.Gk, 85.40.Hp

Manuscript received 17.11.20; revised version received 21.01.21; accepted for publication 10.02.21; published online 09.03.21.

1. Introduction

Discovered in 1974 surface-enhanced Raman scattering (SERS) spectroscopy [1] is a very sensitive analytical method for identifying chemical and biological molecules, and has been intensively developed for more than 40 years [2-10]. The high sensitivity of SERS is increasingly used in characterization of substances in chemistry, physical and biological sciences, environmental monitoring and medical diagnostics, *etc.* [5-7]. The giant enhancement of Raman scattering is explained by interaction of incident light with metallic nanostructures (nanoparticles, nanotips, rough surfaces, laterally ordered relief nanostructures, *etc.*), which leads to a significant increase in the electric field of exciting electromagnetic radiation and the scattered light intensity as a result of exciting the surface plasmons in these

nanostructures (SERS substrates) [2]. As a rule, noble metals like to gold or silver are used for manufacturing SERS substrates. A huge Raman signal amplification factor (up to 10¹⁴) was achieved, and the possibility to detect even single molecules by using these SERS substrates has been demonstrated [8, 9].

Today, many different types of SERS substrates have been proposed, and the methods for their manufacturing can be separated into two classes. The cheapest SERS substrates are made using the methods of chemical synthesis and deposition of metal nanoparticles on substrates, or chemical/electrochemical etching of metal layers [11-13]. However, such substrates, as a rule, exhibit insufficient reproducibility, as well as inhomogeneous signal distribution over the substrate surface, which complicates quantitative measurements and estimates of molecule concentrations.

The second group of methods for manufacturing SERS substrates, which enables to produce periodic uniformly distributed nanostructures with elements of a set shape and size, is associated with the use of modern but rather expensive lithographic technologies: electron-beam lithography [14], ion-beam lithography [15], nano-stamping [16], optical lithography in the far ultraviolet range [17], *etc.* As a result, the cost of these structures is rather high, which prevents their widespread use.

At the same time, interference lithography, which can be used to form ordered metallic nanostructures, is simpler and more technological. In previous studies of the authors [18, 19], it was shown that interference lithography using vacuum chalcogenide glass (CG) photoresists is a promising technology to form one- and two-dimensional submicron periodic structures on the surface of semiconductors and dielectrics, including laterally ordered plasmonic nanostructures, which can be used as SERS substrates.

Another disadvantage of traditional substrates for SERS is the impossibility of registering the full spectrum of high molecular weight compounds due to the fact that not all bonds of these molecules fall into the places of localization of the plasmon excitation field. Large molecules (for example, protein globules) can be oriented in such a way that the bonds under study are not sufficiently close to the surface of the metal nanostructure, and the band corresponding to their vibrations cannot appear in the spectrum [20]. The above problems can be overcome using the so-called "plasmonic nanocavities or antinanostructures" [21]. This opens up the possibility to obtain the SERS spectrum, in which all the bands characteristic of the target molecule are present, since it can be located inside nanocavities and uniformly exposed to the electromagnetic field.

This paper presents the results of development and optimization of the formation processes for SERS substrates in the form of two-dimensional arrays of noble metal nanocavities by using interference photolithography based on a two-layer chalcogenide photoresist.

2. Modeling the distribution of electric field at the surface of nanocavities based on noble metals

Simulation of the distribution of electric field (EF) at the surface of nanostructures was carried out using the COMSOL Multiphysics 5.3a platform (AC/DC module). The wavelengths for this modeling were as follows: 473, 532, 633, 785 and 980 nm. The power density of the incident radiation was 105 W/cm². Modeling was carried out for structures of the following architecture.

1. Nanocavities with a rounded bottom in monocrystalline silicon, the walls and bottom of which were conformally coated with the 100-nm thick silver layer. The distance between nanocavities was 10 nm. The depth and diameter of nanocavities were 0.5 μm .

2. Nanocavities with a rounded bottom in monocrystalline silicon, the walls and bottom of which were

conformally coated with the 20-nm thick silver layer. The distance between nanocavities was 10 nm. The depth and diameter of nanocavities were 0.5 μm .

3. Nanocavities with a rounded bottom in the silver layer. The distance between nanocavities was 10 nm. The depth and diameter of the nanocavities were 0.5 μm .

It should be noted that silver was chosen due to its rather high activity in surface-enhanced Raman scattering spectroscopy in comparison with other metals.

Figs 1 and 2 show the results of modeling the distribution of the electric field in nanocavities. It is seen that the shape of distribution and the magnitude of the EF intensity for nanocavities in silicon coated with the 100-nm thick silver layer and in pure silver practically coincide.

In both cases, upon excitation by radiation with the wavelength 473 nm, no localization of the field is observed at the entrance to the nanocavity, but at the same time, due to internal re-reflections, the field is concentrated in the form of a double "cloud" at the bottom of the channel. The maximum value of the intensity due to the surface plasmon resonance at the entrance to the nanocavity is observed at $\lambda = 532$ nm.

The highest electric field, due to internal re-reflections, is about $2 \cdot 10^3$ V/m in all the nanocavities. This value is practically the same for all the nanocavities in silicon coated with silver and in silver. The geometry of nanocavities has little effect on the maximum value of EF.

The maximum EF in the "cloud", which is formed due to internal re-reflection, shifts from the bottom to the inlet of the nanocavity with an increase in the excitation wavelength from 473 up to 980 nm. Localization of the maximum of EF in the center of nanocavities is observed for 633 and 785 nm.

Similar results were obtained for nanocavities in silicon conformally coated with the 20-nm thick silver layer. The only difference is that, for samples coated with a thinner silver layer, the region of increased EF intensity is somewhat wider diffused inside the volume of nanocavity.

Thus, the simulation results show that nanocavities can be formed in a semiconductor or dielectric layer and then covered with a layer of a plasmon-supporting metal (silver or gold) with the thickness from the range between 20 and 100 nm. In our work, a chalcogenide glassy semiconductor (chalcogenide glass (CG)) was used as a relief-forming layer. The use of nanocavities with the size close to 500 nm or wider in the layers of metals or other materials conformally coated with a metal layer having the thickness from the specified range can make it possible to more efficiently analyze the structure of macromolecules by using surface-enhanced Raman spectroscopy as compared to metal nanoparticles. The macromolecules will be completely covered by the "cloud" inside nanocavities. It should ensure almost uniform excitation of all bonds between atoms, which cannot be achieved when the molecule is located between nanoparticles, where localization of the region of increased EF is limited to a few nanometers.

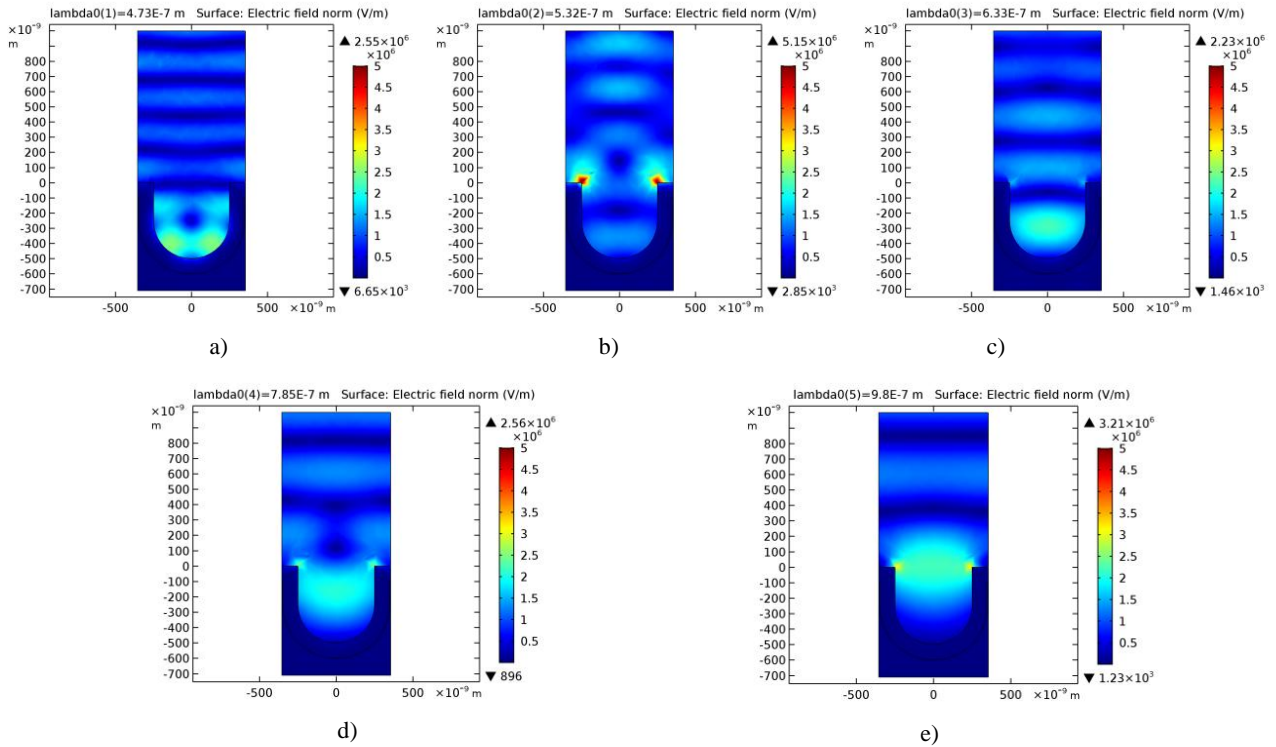


Fig. 1. Distribution of electric field in the silicon-based nanocavities with a rounded bottom, coated with the silver layer 100 nm thick, exposed to electromagnetic radiation with the wavelength 473 nm (a), 532 (b), 633 (c), 785 (d), and 980 (e). Section plane $-yz$.

3. Experimental

To form nanocavities with a deep relief, it was proposed to use a two-layer chalcogenide photoresist consisting of $As_{10}Ge_{30}S_{60}$ and $As_{40}S_{30}Se_{30}$ layers sequentially deposited on a substrate [22]. The top layer $As_{40}S_{30}Se_{30}$ is a high resolution light-sensitive photoresist that can be used to obtain an interference lithographic mask. The $As_{10}Ge_{30}S_{60}$ layer is practically insensitive to light, but mechanically and thermally more stable than $As_{40}S_{30}Se_{30}$. This layer was used to form a matrix of nanocavities of set shapes and sizes in it.

The samples for research were prepared by sequential thermal evaporation in vacuum of $2 \cdot 10^{-3}$ Pa and deposition on a substrate of an adhesive Cr layer with the thickness close to 30 nm, a relief-forming layer of $As_{10}Ge_{30}S_{60}$ with the thickness 300 to 700 nm (depending on the spatial period in the matrix of nanocavities) and a light-sensitive layer of $As_{40}S_{30}Se_{30}$ with the thickness close to 100 nm. Polished glass plates $76 \times 76 \times 2$ mm in size were used as substrates. The thickness control during the deposition of the layers was carried out using the quartz thickness meter (KIT-1), after deposition – with MII-4 microinterferometer.

Recording the interference structures in CG layers was performed using an interference pattern from the radiation of a helium-cadmium laser (wavelength $\lambda = 441.6$ nm) with a given spatial frequency. To record a two-dimensional matrix of nanocavities, the double exposure of the sample was performed, and before the second exposure, the sample was rotated around the

normal to its surface by 90° . The total exposure was $0.2 \dots 0.5$ J/cm². After the double exposure, selective liquid etching of the $As_{40}S_{30}Se_{30}$ layer was carried out to form a lithographic mask with holes (the size of which depended on the etching time) reaching the surface of the $As_{10}Ge_{30}S_{60}$ layer. The next steps of the technical process were exposure of the resulting structure to the integrated radiation of a DKSL-1000 xenon lamp and etching through the lithographic mask of the $As_{10}Ge_{30}S_{60}$ layer. Such exposure before etching of the lower layer has a double positive effect: it strengthens the mask by additional photostimulated polymerization (reduction of defectiveness) of the chalcogenide layer in the mask, and also increases the rate of dissolution of the relief-forming $As_{10}Ge_{30}S_{60}$ layer with a positive etch (photo-stimulated etching). The etchant temperature, concentration of active components in solutions, and etching time define both the parameters of the lithographic mask and the shape of the elements as well as the modulation depth of the resulting nanostructures. The etching of the photoresist and relief-forming layer was controlled *in situ* by recording non-photoactive long-wave light diffracted from the relief structure. After removing the residues of the photoresist, washing, and drying, the formed periodic structure of the cavities in the $As_{10}Ge_{30}S_{60}$ layer was obtained.

A Hitachi-4800 scanning electron microscope and Dimension 3000 Scanning Probe Microscope (Digital Instruments Inc., Tonawanda, NY, USA) were used to determine the profile shape of the relief elements in the

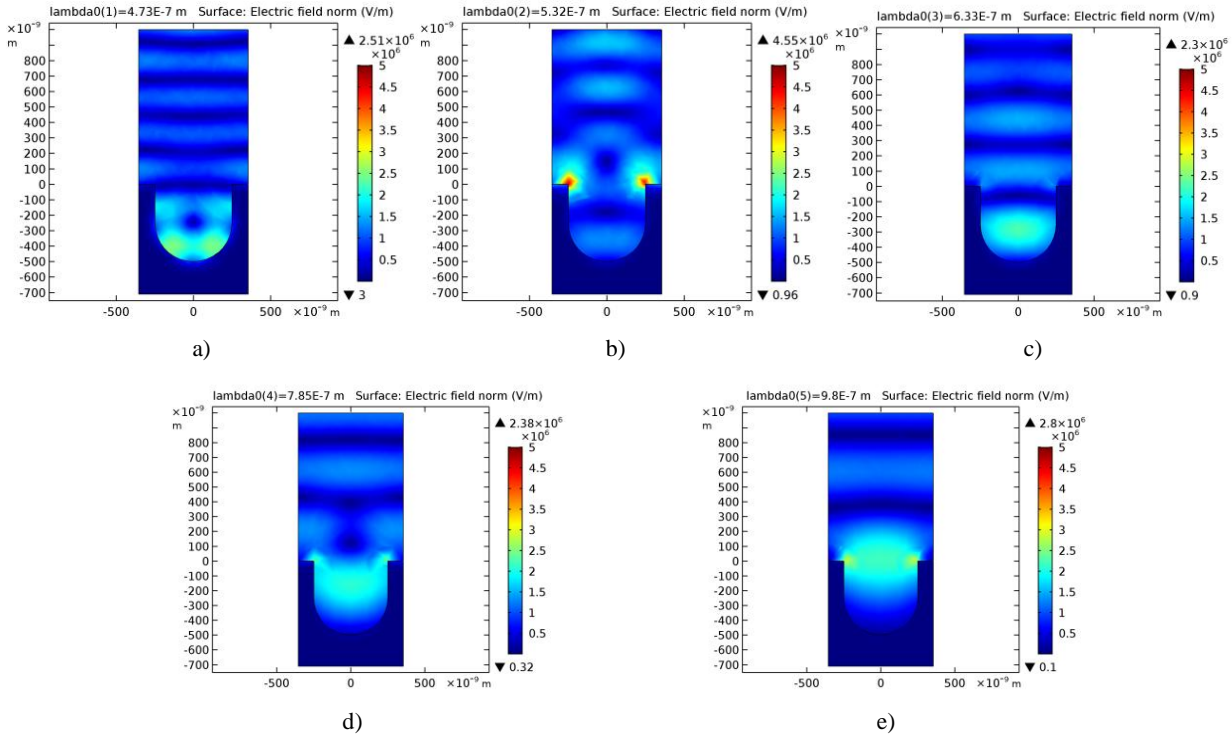


Fig. 2. Distribution of electric field in the silver-based nanocavities with a rounded bottom under action of electromagnetic radiation with the wavelength 473 nm (a), 532 (b), 633 (c), 785 (d), and 980 (e). Section plane $-yz$.

periodic structure and their sizes. The spatial frequency of the nanocavity matrices was determined using the optical stand based on a G5M goniometer with the accuracy ± 3 lines/mm.

To obtain the desired effect from using the two-layer resist, *i.e.*, to create a reliable lithographic mask of the required profile, it is necessary to select not only the composition of corresponding layers, but also the composition of etchants for them. The main requirement in this case was the absence of etching of the $As_{40}S_{30}Se_{30}$ layer when etching the $As_{10}Ge_{30}S_{60}$ layer and *vice versa* – the $As_{10}Ge_{30}S_{60}$ layer should not be dissolved in the etchant for the $As_{40}S_{30}Se_{30}$ photoresist layer. Earlier, a series of studies was carried out on the kinetics of etching of these layers in a number of organic and inorganic etchants for chalcogenide glasses. It was found that the optimal etchant for $As_{40}S_{30}Se_{30}$ is a negative-type organic etchant based on ethylenediamine ($C_2H_8N_2$), and for the relief-forming layer $As_{10}Ge_{30}S_{60}$, an aqueous solution of KOH in the low concentration (0.1%) [22]. The selected anhydrous etchant is characterized by good selectivity for the $As_{40}S_{30}Se_{30}$ layer (the selectivity value, *i.e.*, the ratio of the dissolution rates of unexposed and exposed layers reaches 13) and almost does not dissolve the $As_{10}Ge_{30}S_{60}$ layer. It enables to form an interference relief on the upper light-sensitive layer of $As_{40}S_{30}Se_{30}$. In its turn, the etchant for $As_{10}Ge_{30}S_{60}$ based on 0.1% KOH solution is virtually neutral for compounds based on $As_{40}S_{30}Se_{30}$ without dissolving either the freshly deposited or exposed films of the upper resist layer. At the same time,

the $As_{10}Ge_{30}S_{60}$ layer is dissolved at a high, but controlled, rate, which makes it possible to form a deeper (as compared to the upper layer) relief in the $As_{10}Ge_{30}S_{60}$ film.

To study the SERS activity of arrays of metal nanocavities fabricated using interference lithography in CG and subsequent deposition of metals, a lysozyme (an aqueous solution of lysozyme, concentration 10^{-6} M) was used as an analyte with a high molecular weight. Liquids for analysis were obtained preparing the base 0.01 M solutions by mixing analyte powder with water, which were subsequently diluted to achieve the predetermined concentration. The substrates, on which the arrays of metallized nanocavities were formed, were cut into the samples with dimensions 3×10 mm. Each of the samples was kept for 30 s in the weak solution of hydrochloric acid (4.5%) to remove contaminants on the developed metal surface, which appear as a result of adsorption of organic molecules from the environment. After cleaning, the samples were washed three times in deionized water and twice in ethanol, then immersed in the aqueous solution of lysozyme (concentration 10^{-6} M) and then washed again with deionized water for 10...20 s to remove unadsorbed analyte molecules from their surface.

SERS measurements were carried out using a Confotec® NR500 3D scanning laser Raman microscope equipped with a 633 nm laser. The spectra were recorded by focusing the laser radiation on the sample surface through the $\times 40$ objective. The signal accumulation time was 1 s.

4. Production of experimental samples of SERS substrates

After optimization of the parameters corresponding to the processes of vacuum deposition of layers, interference exposure of the selected two-layer photoresist, post-exposure processing and taking into account the simulation results, prototypes of SERS substrates with different spatial frequencies (from 1200 down to 800 mm^{-1}) and depths of nanocavities (from 250 up to 500 nm) were manufactured.

As an example, Fig. 3 shows a SEM image (section) of this SERS substrate for detecting the Raman spectra of macromolecular compounds. This substrate is a periodic matrix of nanocavities, which is covered with a layer of gold, silver, or a two-layer Ag-Au layer. The period of this matrix is 895 ± 0.5 nm (spatial frequency $\nu = 1117 \text{ mm}^{-1}$). For this period, the initial thickness of the relief-forming layer was 350 nm, and the thickness of the photosensitive layer was 100 nm. The ratio of the cavity depth to its width is slightly higher than 0.4, and the cavity width is about 600 nm, which is close to the values used to simulate the distribution of the electric field.

A similar method was also used to fabricate relief structures with a binary arrangement of cavities with a slightly increased period of matrix – 1207 ± 0.5 nm (spatial frequency $\nu = 829 \text{ mm}^{-1}$). The parameters of layers deposited successively onto a glass substrate for this period were as follows: Cr – 35 nm, $\text{As}_{10}\text{Ge}_{30}\text{S}_{60}$ – 600 nm, $\text{As}_{40}\text{S}_{30}\text{Se}_{30}$ – 100 nm.

When making these samples, we used the repeated exposure by the integrated radiation of the DKSL-1000 lamp during etching of the $\text{As}_{10}\text{Ge}_{30}\text{S}_{60}$ layer. These additional exposures enabled to obtain structures with a higher modulation depth. The samples were also coated with the layers of metals: Al (40 nm), Ag (100 nm), and Au (50 nm) in combinations (Al+Ag) and (Al+Ag+Au).

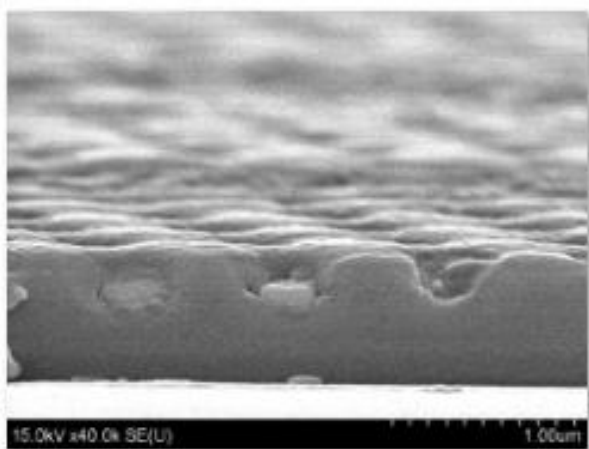


Fig. 3. SEM images (cross-section) a SERS substrate for detecting high-molecular compounds manufactured using the two-layer chalcogenide photoresist.

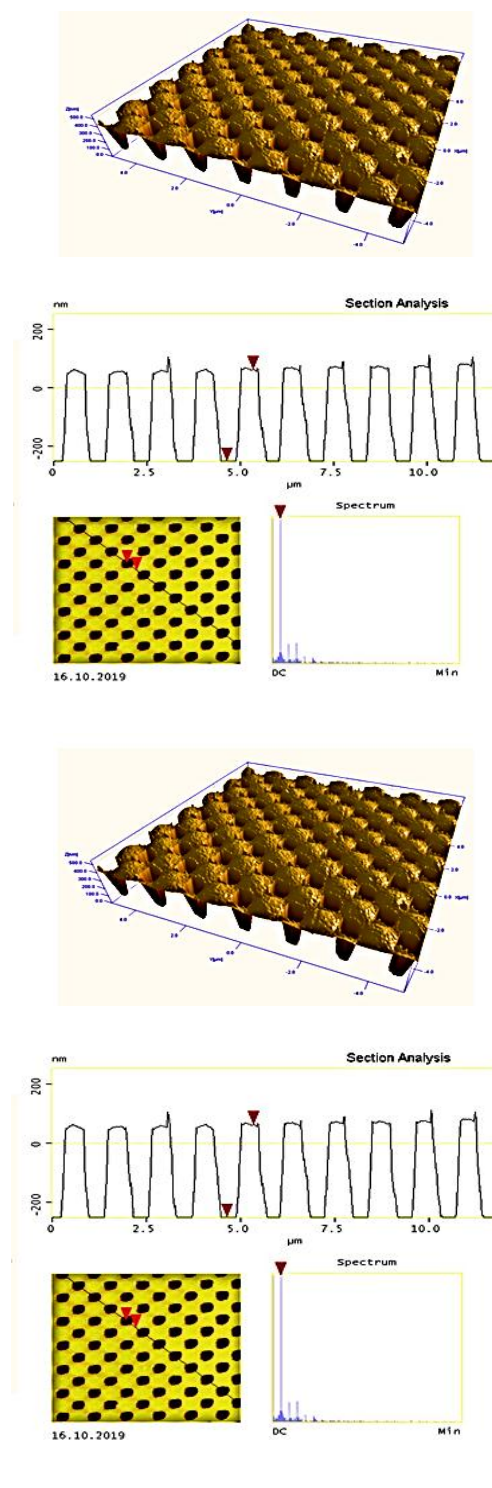


Fig. 4. AFM image and cross-section of a SERS substrate for detecting high-molecular compounds with an increased period and different duty cycle

Figs 4a and 4b show the AFM image, as well as the cross-sectional profiles of two similar SERS substrates with an increased period. Both substrates have the same spatial period equal to 1207 ± 0.5 nm (spatial frequency $\nu = 829 \text{ mm}^{-1}$), but different modulation depths: for the substrate (a), the depth of the cavity was 430 nm, and

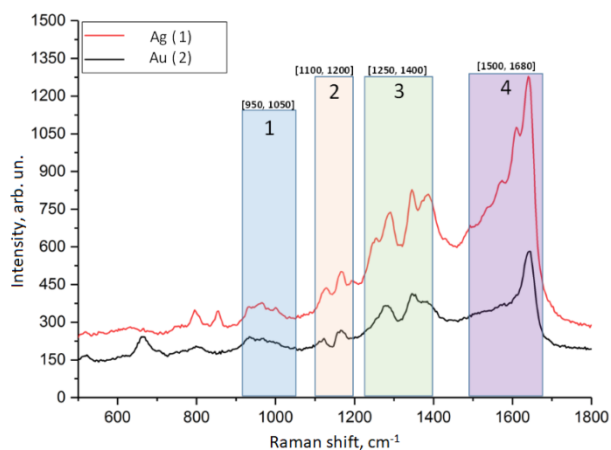


Fig. 5. Average SERS spectra of lysozyme molecules adsorbed on SERS substrates in the form of ordered matrices of nanocavities coated with silver (1) and gold (2) from the solution with the concentration close to 10^{-6} M.

the ratio of the depth of the cavity to its width was 0.57, whereas for the sample (b), the corresponding values were 380 nm and 0.44 nm (remind, that simulation of the distribution of electric field was carried out for the cavities with the depth-to-width ratio close to 0.5). The duty cycle of these two matrices is also different – for the sample (a), the width of cavities on the sample surface was about 750 nm, and for the sample (b), it was 870 nm. These two characteristics can be changed independently of each other: the duty cycle of the matrix is defined mainly by the duty cycle of the lithographic mask, which is formed in the upper layer of the two-layer photoresist (*i.e.*, the time of interference exposure and etching of this layer). And the depth of cavities (and, accordingly, the modulation depth) is defined by the etching time of the relief-forming layer below.

In the course of studies by using the Raman spectrometer, it was found that all substrates exhibit SERS activity. As mentioned above, lysozyme was used as a macromolecular compound. To establish the possibility of obtaining reproducible spectra, each substrate, kept in a lysozyme solution, was scanned using a Confotec Raman spectrometer and a laser with the wavelength 633 nm. It is this radiation that allows location of the “cloud” of electric field at the center of nanocavity with account of the simulation results. The size of the scanning area was $20 \times 20 \mu\text{m}$, the scanning step was $1 \mu\text{m}$. Fig. 5 shows the reproducible SERS spectra of lysozyme, which were obtained using the optimized samples with nanocavities of 750 nm in diameter. Raman spectroscopy provided registration of 28 – 41 SERS spectra of lysozyme out of 400 (Fig. 5), and SERS spectra that have 4 bands typical for proteins were considered as reproducible. As seen from the figure, the SERS signal from lysozyme molecules adsorbed in silver nanocavities was three times higher than that in the gold ones.

5. Conclusions

As a result of numerical simulating the distribution of electric field in nanocavities based on noble metals during the incidence of a light wave and excitation of surface plasmons, it has been ascertained that a region of increased field is formed inside the cavity and, for certain cases, spreads over a considerable part of its volume. This effect is practically identical both for cavities in silver layers and in layers of other substances conformally coated with a silver layer. The use of these nanocavities larger than 500 nm enables to efficiently analyze the structure of macromolecules by using surface-enhanced Raman light scattering spectroscopy, since the macromolecules can completely overlap with regions of increased field inside the nanocavities.

It has been shown that technology of interference lithography based on two-layer chalcogenide photoresists makes it possible to form effective SERS substrates in the form of laterally ordered matrices of nanocavities with specified morphological characteristics (spatial frequency, nanocavity sizes, composition and thickness of a conformal metal coating) for detecting the compounds of high molecular mass, which has been confirmed by registration of reproducible SERS spectra of lysozyme.

Acknowledgements

The work was supported by the Ukrainian-Belarusian project M/42-2020 “New plasmonic nano-materials based on laterally-ordered structures of noble metals for precise, rapid analysis of macromolecular compounds by using spectroscopy of surface-enhanced Raman scattering”.

References

1. Fleischmann M., Hendra P., McQuillan A. Raman spectra of pyridine adsorbed at a silver electrode. *Chem. Phys. Lett.* 1974. **26**. P. 163–166. [https://doi.org/10.1016/0009-2614\(74\)85388-1](https://doi.org/10.1016/0009-2614(74)85388-1).
2. Moskovits M. Surface-enhanced spectroscopy. *Rev. Mod. Phys.* 1985. **57**. P. 783–826.
3. Demirel G., Usta H., Yilmaz M. *et al.* Surface-enhanced Raman spectroscopy (SERS): an adventure from plasmonic metals to organic semiconductors as SERS platforms. *J. Mater. Chem. C*. 2018. **6**, Issue 20. P. 5314–5335. <https://doi.org/10.1039/C8TC01168K>.
4. Schlucker S. Surface-enhanced Raman spectroscopy: concepts and chemical applications. *Angew. Chem. Int. Ed.* 2014. **53**. P. 4756–4795. <https://doi.org/10.1002/anie.201205748>.
5. Ding S.Y., Yi J., Li J.F. *et al.* Nanostructure-based plasmon-enhanced Raman spectroscopy for surface analysis of materials. *Nat. Rev. Mater.* 2016. **1**. P. 1–16. <https://doi.org/10.1038/natrevmats.2016.21>.
6. Wang A.X., Kong X. Review of recent progress of plasmonic materials and nanostructures for surface-enhanced Raman scattering. *Materials*. 2015. **8**, N 6. P. 3024–3052. <https://doi.org/10.3390/ma8063024>.

7. McNay G., Eustace D., Smith W.E., Faulds K., Graham D. Surface-enhanced Raman scattering (SERS) and surface-enhanced resonance Raman scattering (SERRS): A review of applications. *Appl. Spectrosc.* 2011. **65**. P. 825–837. <https://doi.org/10.1366/11-06365>.
8. Nie S., Emory S.R. Probing single molecules and single nanoparticles by surface-enhanced Raman scattering. *Science*. 1997. **275**. P. 1102–1106. <https://doi.org/10.1126/science.275.5303.1102>.
9. Kneipp K., Wang Y., Kneipp H. *et al.* Single molecule detection using surface-enhanced Raman scattering (SERS). *Phys. Rev. Lett.* 1997. **78**. P. 1667. <https://doi.org/10.1103/PhysRevLett.78.1667>.
10. Sharma B., Frontiera R.R., Henry A.I., Ringe E., van Duyne R.P. SERS: Materials, applications, and the future. *Mater. Today*. 2012. **15**, No 1–2. P. 16–25. [https://doi.org/10.1016/S1369-7021\(12\)70017-2](https://doi.org/10.1016/S1369-7021(12)70017-2).
11. Wei H., Xu H.X. Hot spots in different metal nanostructures for plasmon-enhanced Raman spectroscopy. *Nanoscale*. 2013. **5**, No 22. P. 10794–10805. <https://doi.org/10.1039/c3nr02924g>.
12. Banholzer M.J., Millstone J.E., Qin L.D., Mirkin C.A. Rationally designed nanostructures for surface-enhanced Raman spectroscopy. *Chem. Soc. Rev.* 2008. **37**. P. 885–897. <https://doi.org/10.1039/b710915f>.
13. Fan M.K., Andrade G.F.S., Brolo A.G. A review on the fabrication of substrates for surface enhanced Raman spectroscopy and their applications in analytical chemistry. *Anal. Chim. Acta*. 2011. **693**, No 1-2. P. 7–25. <https://doi.org/10.1016/j.aca.2011.03.002>.
14. Yue W., Wang Z., Yang Y., Chen, L., Syed A., Wong K., Wang X. Electron-beam lithography of gold nanostructures for surface-enhanced Raman scattering. *J. Micromech. Microeng.* 2012. **22**, No 12. P. 125007. <https://doi.org/10.1088/0960-1317/22/12/125007>.
15. Lin Y.Y., Liao J.D., Ju Y.H., Chang C.W., Shiau A.L. Focused ion beam-fabricated Au micro/nanostructures used as a surface enhanced Raman scattering-active substrate for trace detection of molecules and influenza virus. *Nanotechnology*. 2011. **22**, No 18. P. 185308. <https://doi.org/10.1088/0957-4484/22/18/185308>.
16. Barbillon G., Hamouda F., Held S., Gogol P., Bartenlian B. Gold nanoparticles by soft UV nanoimprint lithography coupled to a lift-off process for plasmonic sensing of antibodies. *Microelectron. Eng.* 2010. **87**. P. 1001–1004. <https://doi.org/10.1016/j.mee.2009.11.114>.
17. Mandal P., Gupta P., Nandi A., Ramakrishna S.A. Surface enhanced fluorescence and imaging with plasmon near-fields in gold corrugated gratings. *J. Nanophotonics*. 2012. **6**, No 1. P. 063527. <https://doi.org/10.1117/1.JNP.6.063527>.
18. Dan'ko V., Indutnyi I., Min'ko V., Shepelyavyi P. Interference photolithography with the use of resists on the basis of chalcogenide glassy semiconductors. *Optoelectronics Instrum. Data Process.* 2010. **46**, No 3. P. 483–490. 10.3103/S8756699011050116.
19. Dan'ko V., Dmitruk M., Indutnyi I. *et al.* Fabrication of periodic plasmonic structures using interference lithography and chalcogenide photoresist. *Nanoscale Res. Lett.* 2015. **10**. P. 497. <https://doi.org/10.1186/s11671-015-1203-x>.
20. Arzumanyan G., Doroshkevich N., Mamatkulov K. *et al.* Phospholipid detection by surface-enhanced Raman scattering using silvered porous silicon substrates. *phys. status solidi (a)*. 2017. **214**, No 8. P. 1600915. <https://doi.org/10.1002/pssa.201600915>.
21. Kelf T.A., Sugawara Y., Cole R.M., Baumberg J.J. Localized and delocalized plasmons in metallic nanowires. *Phys. Rev. B*. 2006. **74**, No 24. P. 245415. <https://doi.org/10.1103/PhysRevB.74.245415>.
22. Indutnyi I.Z., Dan'ko V.A., Myn'ko V.I. *et al.* Spatial frequency doubling of interference lithographic structure using two-layer chalcogenide photoresist. *J. Optoelectron. Adv. Mater.* 2011. **13**, No. 11-12. P. 1467–1469.

Authors and CV



Viktor A. Dan'ko, Doctor of Physics and Mathematics, Head of the Laboratory of interference lithography at the V. Lashkaryov Institute of Semiconductor Physics, NASU. His main research activity is in the field of optics of thin films, photo-stimulated processes in thin film structures, nanoparticles and nanostructures, interference lithography. He is the author of more than 150 publications, 9 patents.



Ivan Z. Indutnyi, Doctor of Physics and Mathematics, Professor, Chief Researcher of the Laboratory of interference lithography at the V. Lashkaryov Institute of Semiconductor Physics, NASU. His main research activity is in the field of optics of thin films, photostimulated processes in solids and onto surfaces, nanoparticles and nanostructures, interference lithography, plasmonics and sensing. He is the author of more than 300 publications, 35 author's certificates and patents.



Viktor I. Myn'ko, PhD in Physics and Mathematics, Senior Scientific Researcher of the Laboratory of interference lithography. The area of his scientific interests: inorganic resists and their application in lithography, holography, optical engineering and information storage. He is the author of more 170 scientific publications, including 1 monograph and 14 author's certificates and patents.



Hanna Bandarenka is a head of the laboratory “Applied Plasmonics” and Associate Prof. at the Belarusian State University of Informatics and Radioelectronics (Minsk, Belarus) where in 2014 she defended her PhD thesis in Engineering Sciences. She is also a Fulbright Prof. in Polytechnic

school of Arizona State University (AZ, USA). The research interest is revealing process-structure-properties relationship of novel plasmonic nanomaterials based on metal-coated nanovoids in silicon and polymers. She has published over 120 scientific papers.



Alexey Dolgiy is a senior research scientist in the laboratory “Applied Plasmonics” at the Belarusian State University of Informatics and Radioelectronics (Minsk, Belarus). He has been focused on design, fabrication and characterization of nanomaterials based on meso- and macroporous

silicon filled/coated with copper, magnetic or noble metals for MEMS, sensors, micro- and optoelectronic devices, microthrusters, *etc.* He is author of more than 20 papers in scientific journals and books.



Petro M. Lytvyn, PhD in Physics and Mathematics, Senior Researcher of the Laboratory of electron probe methods of structural and elemental analysis of semiconductor materials and systems, V. Lashkaryov Institute of Semiconductor Physics, NASU. The area of scientific interests covers nano-

physics of semiconductors and related materials.



Mariia V. Lukaniuk, PhD in Physics and Mathematics. She is Junior Researcher of the Laboratory of interference lithography at the V. Lashkaryov Institute of Semiconductor Physics. She is the author of 33 publications. Her main research activity is related to lithography, chalcogenide vitreous semiconductors and photoresists.



Sergey Redko is a senior research scientist of the laboratory “Materials and Structures of Nanoelectronics” at the Belarusian State University of Informatics and Radioelectronics (Minsk, Belarus). His research interests include the experimental and theoretical study of silicon-based nanostructures

for MEMS, sensors and microthrusters. His publication record includes over 30 papers in scientific journals and books.

Формування латерально упорядкованих масивів нанопорожнин благородних металів для SERS підкладок з використанням інтерференційної фотолітографії

В.А. Данько, І.З. Індутний, В.І. Мінько, П.М. Литвин, М.В. Луканюк, Г.В. Бандаренка, А.Л. Долгий, С.В. Редько

Анотація. Недоліком традиційних SERS підкладок є неможливість зареєструвати повністю спектр високомолекулярних сполук у зв'язку з тим, що не всі зв'язки такої молекули потрапляють у місця локалізації поля плазмонного збудження. Зазначену проблему можна подолати шляхом використання так званих плазмонних нанопорожнин або антинаночастинок. З метою створення SERS підкладок у вигляді нанопорожнин в роботі проведено моделювання розподілу напруженості електричного поля біля поверхні наноструктур (нанопорожнин). Результати моделювання показали, що порожнини можна формувати в шарі напівпровідника або діелектрика і потім покривати шаром плазмон-несучого металу (срібла або золота) товщиною 20–100 нм. У роботі як рельєфоутворюючий шар використовується халькогенідне скло. Наведено результати розробки та оптимізації процесів формування SERS підкладок у вигляді двовимірних масивів нанопорожнин благородних металів з використанням інтерференційної фотолітографії на основі двошарового халькогенідного фоторезисту. Показано, що технологія інтерференційної літографії з використанням двошарового халькогенідного фоторезисту дозволяє формувати ефективні SERS підкладки у вигляді латерально впорядкованих матриць нанопорожнин із заданими морфологічними характеристиками (просторовою частотою, розмірами нанопорожнин, складом та товщиною конформного металічного покриття) для детектування раманівського спектра високомолекулярних сполук, що, зокрема, підтверджується реєстрацією відтворених SERS спектрів молекул лізоциму.

Ключові слова: SERS підкладки, інтерференційна літографія, халькогенідний фоторезист, раманівська спектроскопія.